unless otherwise noted. TPM video-enhanced light microscopy, image recording, image processing and data analysis have been described[5–7]. TPM image acquisition time was 0.5 s.

### χ-Recognition efficiency

The DNA substrates were made by treating *Nde*I-linearized pBR322 or pBR322 3χF, 3H with calf intestinal phosphatase, followed by 5′-end labelling using T4 polynucleotide kinase and [γ-$^{32}$P]ATP. Reactions were conducted at 25 °C essentially as described[20] and contained 25 mM Tris-acetate (pH 7.5), 1 mM $Mg(OAc)_2$, 1 mM DTT, 1 mM ATP, 1 mM ADP, 1.44 nM duplex DNA ends, 1.27 μM SSB and 0.4 nM active RecBCD-bio. The gels were dried then analysed on a phosphor imager; $\chi_3$ recognition efficiency was taken to be the maximum value over measurements taken at different times of $2P_t/(R_0 - R_t)$ where $R_t$ and $P_t$ are the total radioactivity over background at time $t$ in the unprocessed duplex substrate band and the long χ-specific product bands, respectively. This calculation underestimates the true recognition efficiency because an unknown fraction of the χ-specific products are further degraded during the reaction.

Received 23 August; accepted 7 November 2000.


1. Kuzminov, A. Recombinational repair of DNA damage in *Escherichia coli* and bacteriophage lambda. *Microbiol. Mol. Biol. Rev.* **63,** 751–813 (1999).
2. Kowalczykowski, S. C., Dixon, D. A., Eggleston, A. K., Lauder, S. D. & Rehrauer, W. M. Biochemistry of homologous recombination in *Escherichia coli. Microbiol. Rev.* **58,** 401–465 (1994).
3. Gelles, J. & Landick, R. RNA polymerase as a molecular motor. *Cell* **93,** 13–16 (1998).
4. Lovett, S. T., Luisi-DeLuca, C. & Kolodner, R. D. The genetic dependence of recombination in recD mutants of *Escherichia coli*. *Genetics* **120,** 37–45 (1988).
5. Schafer, D. A., Gelles, J., Sheetz, M. P. & Landick, R. Transcription by single molecules of RNA polymerase observed by light microscopy. *Nature* **352,** 444–448 (1991).
6. Yin, H., Landick, R. & Gelles, J. Tethered particle motion method for studying transcript elongation by a single RNA polymerase molecule. *Biophys J.* **67,** 2468–2478 (1994).
7. Finzi, L. & Gelles, J. Measurement of lactose repressor-mediated loop formation and breakdown in single DNA molecules. *Science* **267,** 378–380 (1995).
8. Roman, L. J. & Kowalczykowski, S. C. Characterization of the adenosinetriphosphatase activity of the *Escherichia coli* RecBCD enzyme: relationship of ATP hydrolysis to the unwinding of duplex DNA. *Biochemistry* **28,** 2873–2881 (1989).
9. Roman, L. J. & Kowalczykowski, S. C. Characterization of the helicase activity of the *Escherichia coli* RecBCD enzyme using a novel helicase assay. *Biochemistry* **28,** 2863–2873 (1989).
10. Okada, Y. & Hirokawa, N. A processive single-headed motor: kinesin superfamily protein KIF1A. *Science* **283,** 1152–1157 (1999).
11. Svoboda, K., Schmidt, C. F., Schnapp, B. J. & Block, S. M. Direct observation of kinesin stepping by optical trapping interferometry. *Nature* **365,** 721–727 (1993).
12. Guajardo, R. & Sousa, R. A model for the mechanism of polymerase translocation. *J. Mol. Biol.* **265,** 8-19 (1997).
13. Thaler, D. S. *et al.* in *Mechanisms and Consequences of DNA Damage Processing* (eds Friedberg, E. & Hanawalt, P.) 413–422 (Alan. R. Liss, New York, 1988).
14. Dixon, D. A., Churchill, J. J. & Kowalczykowski, S. C. Reversible inactivation of the *Escherichia coli* RecBCD enzyme by the recombination hotspot chi in vitro: evidence for functional inactivation or loss of the RecD subunit. *Proc. Natl Acad. Sci. USA* **91,** 2980–2984 (1994).
15. Myers, R. S., Kuzminov, A. & Stahl, F. W. The recombination hot spot chi activates RecBCD recombination by converting *Escherichia coli* to a recD mutant phenocopy. *Proc. Natl Acad. Sci. USA* **92,** 6244–6248 (1995).
16. Stahl, F. W., Thomason, L. C., Siddiqi, I. & Stahl, M. M. Further tests of a recombination model in which chi removes the RecD subunit from the RecBCD enzyme of *Escherichia coli. Genetics* **126,** 519–533 (1990); erratum *ibid.* **135,** 1232 (1993).
17. Taylor, A. F. & Smith, G. R. Regulation of homologous recombination: Chi inactivates RecBCD enzyme by disassembly of the three subunits. *Genes Dev.* **13,** 890–900 (1999).
18. Koppen, A., Krobitsch, S., Thoms, B. & Wackernagel, W. Interaction with the recombination hot spot chi in vivo converts the RecBCD enzyme of *Escherichia coli* into a chi-independent recombinase by inactivation of the RecD subunit. *Proc. Natl Acad. Sci. USA* **92,** 6249–6253 (1995).
19. Anderson, D. G., Churchill, J. J. & Kowalczykowski, S. C. Chi-activated RecBCD enzyme possesses 5′→3′ nucleolytic activity, but RecBC enzyme does not: evidence suggesting that the alteration induced by Chi is not simply ejection of the RecD subunit. *Genes Cells* **2,** 117–128 (1997).
20. Dixon, D. A. & Kowalczykowski, S. C. The recombination hotspot chi is a regulatory sequence that acts by attenuating the nuclease activity of the *E. coli* RecBCD enzyme. *Cell* **73,** 87–96 (1993).
21. Roman, L. J., Eggleston, A. K. & Kowalczykowski, S. C. Processivity of the DNA helicase activity of *Escherichia coli* recBCD enzyme. *J. Biol. Chem.* **267,** 4207–4214 (1992).
22. Taylor, A. F., Schultz, D. W., Ponticelli, A. S. & Smith, G. R. RecBC enzyme nicking at Chi sites during DNA unwinding: location and orientation-dependence of the cutting. *Cell* **41,** 153–163 (1985).
23. Cronan, J. E. Jr Biotination of proteins in vivo. A post-translational modification to label, purify, and study proteins. *J. Biol. Chem.* **265,** 10327–10333 (1990).
24. Boehmer, P. E. & Emmerson, P. T. *Escherichia coli* RecBCD enzyme: inducible overproduction and reconstitution of the ATP-dependent deoxyribonuclease from purified subunits. *Gene* **102,** 1–6 (1991).
25. Eichler, D. C. & Lehman, I. R. On the role of ATP in phosphodiester bond hydrolysis catalyzed by the recBC deoxyribonuclease of *Escherichia coli. J. Biol. Chem.* **252,** 499–503 (1977).
26. Young, E. C., Berliner, E., Mahtani, H. K., Perez-Ramirez, B. & Gelles, J. Subunit interactions in dimeric kinesin heavy chain derivatives that lack the kinesin rod. *J. Biol. Chem.* **270,** 3926–3931 (1995).
27. Berliner, E. *et al.* Microtubule movement by a biotinated kinesin bound to streptavidin-coated surface. *J. Biol. Chem.* **269,** 8610–8615 (1994); erratum *ibid.* **269,** 23382 (1994).
28. Anderson, D. G., Churchill, J. J. & Kowalczykowski, S. C. A single mutation, RecB(D1080A) eliminates RecA protein loading but not Chi recognition by RecBCD enzyme. *J. Biol. Chem.* **274,** 27139–27144 (1999).
29. Berliner, E., Young, E. C., Anderson, K., Mahtani, H. K. & Gelles, J. Failure of a single-headed kinesin to track parallel to microtubule protofilaments. *Nature* **373,** 718–721 (1995).
30. Taylor, A. F. & Smith, G. R. Strand specificity of nicking of DNA at Chi sites by RecBCD enzyme. Modulation by ATP and magnesium levels. *J. Biol. Chem.* **270,** 24459–24467 (1995).


**Supplementary information** is available on *Nature*'s World-Wide Web site (http://www.nature.com).


### Acknowledgements

We thank P. Bianco, P. Boehmer, S. Kowalczykowski, S. Lovett and A. Taylor for materials and helpful advice. This work was supported by the NIGMS.


Correspondence and requests for materials should be addressed to J.G. (e-mail: gelles@brandeis.edu).

# Processive translocation and DNA unwinding by individual RecBCD enzyme molecules

**Piero R. Bianco*†, Laurence R. Brewer‡, Michele Corzett§, Rod Balhorn§, Yin Yeh‖, Stephen C. Kowalczykowski*† & Ronald J. Baskin†**

*Sections of * Microbiology and of † Molecular and Cellular Biology and ‖ Department of Applied Science, University of California at Davis, Davis, California 95616, USA*
*‡ Electronics Engineering Technologies Division, and § Biology and Biotechnology Research Program, Lawrence Livermore National Laboratory, Livermore, California 94550, USA*

**RecBCD enzyme is a processive DNA helicase[1] and nuclease[2] that participates in the repair of chromosomal DNA through homologous recombination[3,4]. We have visualized directly the movement of individual RecBCD enzymes on single molecules of double-stranded DNA (dsDNA). Detection involves the optical trapping of solitary, fluorescently tagged dsDNA molecules that are attached to polystyrene beads, and their visualization by fluorescence microscopy[5,6]. Both helicase translocation and DNA unwinding are monitored by the displacement of fluorescent dye from the DNA by the enzyme[7]. Here we show that unwinding is both continuous and processive, occurring at a maximum rate of 972 ± 172 base pairs per second (0.30 μm $s^{-1}$), with as many as 42,300 base pairs of dsDNA unwound by a single RecBCD enzyme molecule. The mean behaviour of the individual RecBCD enzyme molecules corresponds to that observed in bulk solution.**

Visualization of translocation and DNA unwinding by single DNA helicase molecules permits study of the stochastic properties of individual molecular motors, or 'nano-machines', which are obscured in the population average of steady-state, bulk-phase measurements. To achieve such visualization, we manipulated individual, fluorescently labelled DNA molecules by using an optical trap, and detected their unwinding by RecBCD enzyme. DNA substrates were constructed by attaching a biotinylated oligonucleotide to one cohesive end of lambda (λ) DNA. These DNA molecules were attached at low density to 1-μm streptavidin-coated, polystyrene beads. The fluorescent dye YOYO-1 was bound to the DNA, and then RecBCD enzyme was bound to these fluorescent DNA molecules in the absence of ATP. Under these conditions, RecBCD enzyme binds only to the free end of the dsDNA, and neither translocates nor unwinds the DNA until ATP is introduced[8].

These helicase–DNA complexes were introduced into one channel of a Y-shaped, micro-machined flow cell (Fig. 1a; and ref. 6). Helicase reaction buffer containing ATP was introduced into the second channel under conditions of laminar flow, creating a situation in

which the two solutions flowed parallel to one another with negligible mixing. The optically trapped bead appeared as a white sphere (the result of nonspecific binding of YOYO-1 to the bead), with an attached fluorescent DNA 'string' caused by flow-induced extension of the DNA molecule away from the trapped bead[5,6]. Once a RecBCD enzyme–DNA–bead complex was trapped, the stage was moved to reposition this complex, from the sample side of the flow cell across the flow boundary between solutions to the reaction side. If a RecBCD enzyme molecule is attached at the end opposite to the bead, then DNA unwinding will proceed from that end towards the bead, resulting in a decreased length of duplex DNA owing to concomitant unwinding of the dsDNA and displacement of YOYO-1 molecules by a single translocating RecBCD enzyme; the displaced free dye molecules possess negligible solution fluorescence (Fig. 1).

The observed unwinding of individual DNA molecules is shown in Fig. 2. Sequential video frames from representative reactions in the presence and absence of ATP are shown in Fig. 2a and b, respectively (see Supplementary Information). Before movement of the bead with the attached RecBCD–DNA complex to the reaction (ATP) side of the flow cell, the length of the DNA remains constant (first ~18 s of Fig. 2c). On relocation to the reaction side of the flow cell, a rapid decrease (0.145 μm $s^{-1}$) in the DNA length is observed when 1 mM ATP is present. DNA shortening is linear and constant, with no discernible pauses for a period of ~56 s, at which point the change in DNA length stops abruptly. (The occasional instantaneous deviation of DNA length from the average linear behaviour arises from movement of DNA slightly in and out of the focal plane; similar behaviour is observed for experiments either with or without ATP). The length remains constant for the remaining 42 s of this time course, suggesting that the cessation of unwinding results from dissociation of RecBCD enzyme from the remaining dsDNA.

The observed rate of DNA shortening (from $t = 18$ s to $t = 74$ s) corresponds to an apparent rate of DNA helicase movement of 471 ± 30 base pairs (bp) $s^{-1}$ (see Methods). The change in length of dsDNA that occurs before RecBCD enzyme dissociates, 8.3 μm, corresponds to 26,800 ± 700 bp unwound by the single RecBCD enzyme. In contrast, in the absence of ATP there is only a small decrease in the apparent length of the DNA (~ 1 μm) at a rate that is 16-fold lower than the ATP-dependent reaction (−0.009 μm $s^{-1}$ versus −0.145 μm $s^{-1}$). This change in apparent length is enzyme-independent, and results from a slow dissociation of YOYO-1 from sites across the entire length of the DNA molecule that occurs when the DNA molecule is relocated from the sample to the reaction side of the flow cell, owing to the lower YOYO-1 concentration on the reaction side (Fig. 2b; and data not shown). Control experiments done in the presence of ATP, but in the absence of enzyme, produced results identical to those obtained in the absence of ATP (data not shown) and showed that, at longer times, a new equilibrium DNA length was achieved (YOYO-1 elongates dsDNA by 1.1–1.2-fold; refs 5, 6, 9). When the unwinding rate in the presence of 1 mM ATP is corrected for the enzyme-free dissociation of YOYO-1, the corrected unwinding rate ($k_{cat}^{corr}$) is 443 ± 30 bp $s^{-1}$. We conclude that this unwinding rate is due to a single molecule of RecBCD enzyme that bound to the free dsDNA end opposite the bead, and both translocated and unwound the DNA in an ATP-dependent manner once the DNA entered the ATP channel. Additional RecBCD enzyme molecules could not have contributed to the unwinding because RecBCD enzyme binds only to blunt, or nearly blunt dsDNA ends, with a greater than 1 million-fold preference relative to internal sites[10,11], and RecBCD enzyme was present only in the sample side of the flow cell.

To confirm further that the unwinding observed was dependent on RecBCD enzyme, we carried out assays at four additional ATP concentrations and also at 37 °C, because previous steady-state kinetic assays showed that the rate of unwinding depends on both of these variables[11,12]. As expected, the observed rate of unwinding increased with increasing ATP concentration (Fig. 3). In all cases,

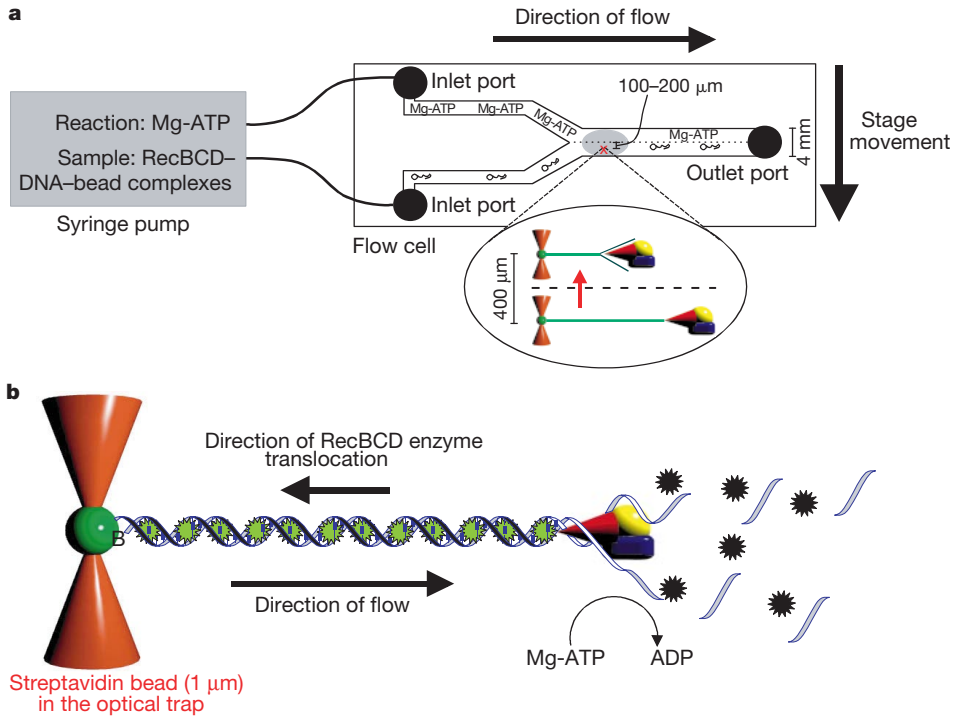


**Figure 1** Visualization of DNA helicase action on individual DNA molecules. **a**, Syringe pump and flow cell: the sample syringe contains helicase–DNA–bead complexes, and the reaction syringe contains ATP. 'X' indicates the laser trap position, and the red arrow indicates movement of the trapped DNA–bead complex across the boundary between solutions. Inset, the trapped DNA with bound helicase, and its unwinding after relocation into the reaction solution. **b**, Fluorescent DNA helicase assay[7]. A trapped and stretched, fluorescent DNA molecule is shown. As RecBCD enzyme translocates, it both unwinds and degrades the DNA, simultaneously displacing dye molecules (black stars). B, biotinylated oligonucleotide.

unwinding of dsDNA molecules was continuous and without any detectable pausing, indicating that the helicase action of individual RecBCD enzymes was not affected detectably by any sequence present in the λ DNA. Microscopic pausing, at the individual base-pair level, would not be detected in our experiments because this is beyond the temporal (33 ms per frame; hence pauses shorter than about 10 frames, or ~330 ms, would be difficult to detect) and spatial resolution of the assay system (a maximum of ~244 nm or 800 bp but, owing to occasional movement of the DNA out of the focal plane, the actual resolution is lower, ~1 μm or ~3,000 bp). Hence, there is no class of limited (10–20) specific pause sites at which the enzyme pauses for more than a fraction of a second or so.

Although the rate of DNA unwinding by any individual RecBCD enzyme molecule was uniform (within experimental error) on any given DNA molecule (Fig. 2), the rate for different helicase molecules deviated by 1.4–5-fold at each ATP concentration examined (Fig. 3). However, their average behaviour at each ATP concentration was similar to that observed in both steady-state solution experiments[1,11] and electron microscopic assays that analysed intermediates of the unwinding reaction[13]. For example, at 250 μM ATP

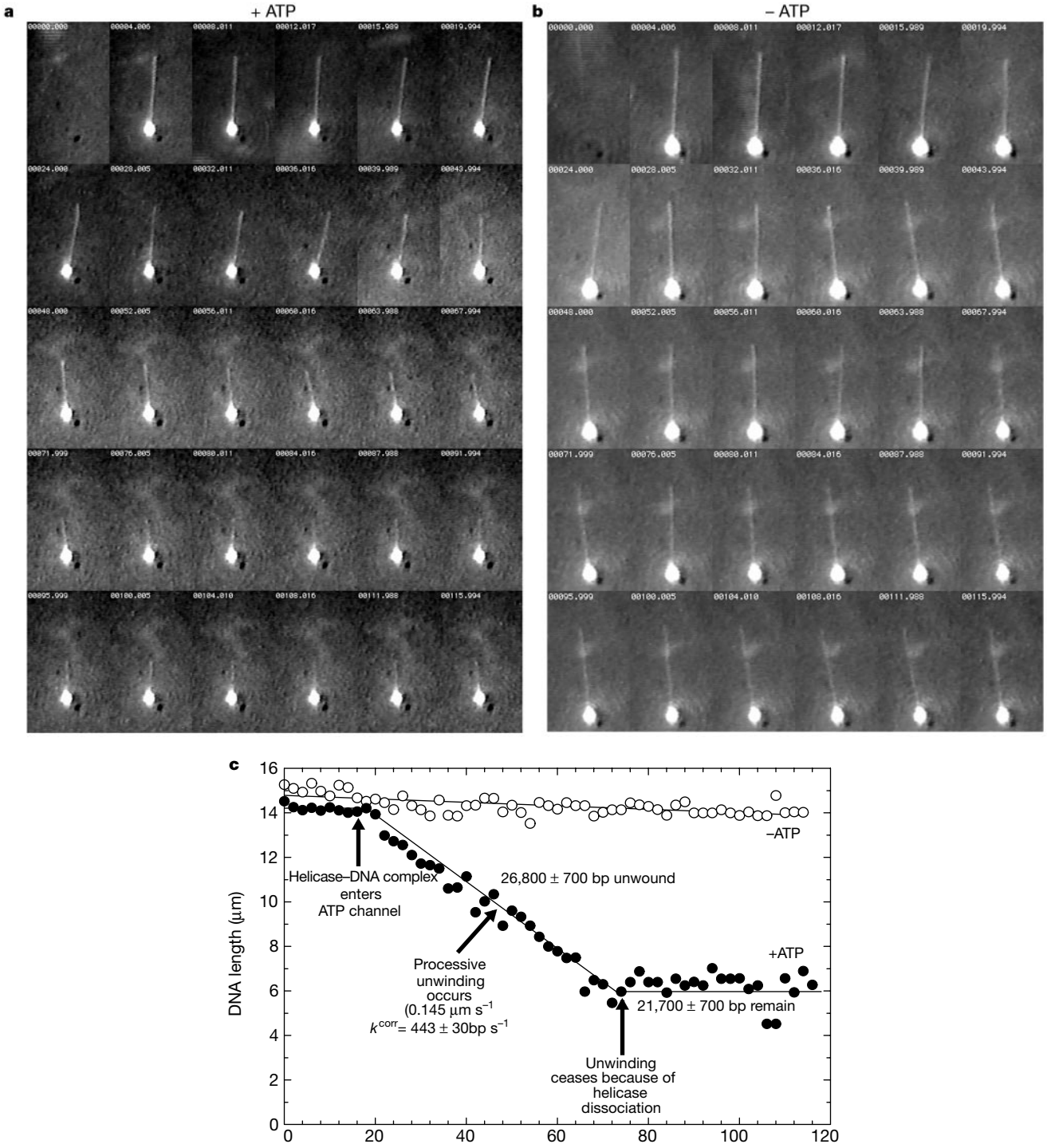


**Figure 2** Unwinding of a DNA molecule by RecBCD enzyme. **a**, **b**, Selected, sequential frames from a video recording of reactions either in the presence (**a**) or absence (**b**) of ATP (1 mM). The direction of translocation and DNA unwinding by RecBCD enzyme is from the DNA end opposite the bead, towards the bead (that is, from the top of each frame towards the bottom). Numbers at the top of each frame indicate elapsed time. **c**, Analysis of the time courses in **a** and **b**.

the unwinding rate for eight individual enzymes varied from a minimum of 156 bp $s^{-1}$ to a maximum of 428 bp $s^{-1}$, with an average of 359 ± 89 bp $s^{-1}$. A similar behaviour was observed at each of the four additional ATP concentrations used. Both this variation in unwinding rate by individual helicase molecules and the unfaltering movement could not have been discerned from steady-state experiments. At present, the source of this variation is unknown; some of the variation might be day-to-day variation or variation in the DNA–bead preparation used, but at least a twofold variance was observed for six molecules on the same day with the same DNA–bead preparation. Variation in individual enzymatic activity was observed for at least two other enzymes: lactate dehydrogenase[14] and T7 DNA polymerase[15]. Despite the individual variation, when the averaged data from the unwinding of 42 DNA molecules (Fig. 3a) were fitted to the Michaelis–Menten equation, a $V_{max}$ of 521 ± 60 bp $s^{-1}$ and a $K_m^{ATP}$ of 142 ± 58 μM was obtained. Both values are virtually identical to those reported from bulk-solution experiments (586 ± 45 bp $s^{-1}$ and 130 ± 30 μM ATP, respectively[11,12,16]). In addition to being dependent on ATP concentration, the rate of unwinding in 1 mM ATP increased twofold when the temperature was raised to 37 °C (Table 1); this $k_{cat}^{corr}$ (972 ± 172 bp $s^{-1}$) is essentially identical to that obtained from steady-state measurements (930 ± 15 bp $s^{-1}$; ref. 11).

In addition to obtaining dsDNA unwinding rates, we directly observed the distance travelled by an individual RecBCD enzyme from its binding site at a dsDNA end to its point of dissociation, a distance that directly defines the processivity of DNA unwinding (that is, the number of base pairs unwound by a single helicase molecule per DNA binding event before dissociation) (Fig. 3b and Table 1). The processivity varied in an ATP-dependent fashion, with the maximum value observed at 1 mM ATP. There was a stochastic variation in the processivity of individual RecBCD enzyme molecules at any given ATP concentration (Fig. 3b). For example, at 250 μM ATP, unwinding terminated abruptly after values ranging from 9,200 to 39,500 bp of dsDNA unwound by eight different RecBCD enzymes. The average value is 22,900 ± 9,500 bp, which is similar to that determined previously (27,000 ± 3,000 bp; ref. 1).

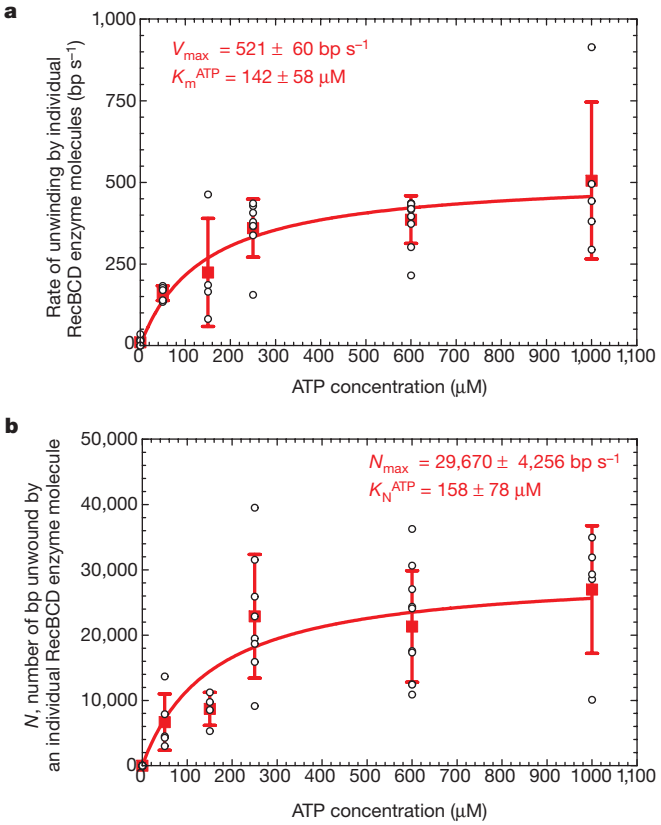


**Figure 3** Both the rate and processivity for dsDNA unwinding by individual RecBCD enzyme molecules may vary, but their averages fall within ranges observed for bulk solution. For each ATP concentration (23 °C), 4–10 DNA molecules were measured on different days, using several different preparations. **a**, Unwinding rates for single RecBCD enzyme molecules; **b**, processivities for the same molecules. Open circles represent individual molecule results, and squares represent their average for a given ATP concentration (error bars indicate the standard deviation). Data were fitted to a hyperbola (red line) for comparison with previously published steady-state values[1].

**Table 1 Summary of DNA helicase behaviour for individual RecBCD enzymes**

| Temperature (°C) | ATP concentration (mM) | $k_{cat}^{corr.}$ (bp $s^{-1}$ per RecBCD)* | *N* (bp per end)† |
|---|---|---|---|
| 23 | 0.05 | 161 ± 23 (5)‡ | 6,700 ± 4,300 |
| 23 | 0.15 | 224 ± 166 (4) | 9,600 ± 3,000 |
| 23 | 0.25 | 359 ± 89 (8) | 22,900 ± 9,500 |
| 23 | 0.60 | 386 ± 71 (10) | 21,300 ± 8,500 |
| 23 | 1.00 | 502 ± 243 (5) | 27,000 ± 9,800 |
| 37 | 1.00 | 972 ± 172 (3) | 38,000 ± 5,700 |

*The observed unwinding rate as calculated for the linear portion of plots such as those shown in Fig. 2c. As the rate is determined from an individual enzyme molecule, we refer to it as $k_{cat}$; it has been corrected for the ATP-independent rate, thus $k_{cat}^{corr}$. The observed variation is the standard deviation of unwinding rates for individual RecBCD enzyme molecules at that ATP concentration.
†*N* is the number of base pairs of dsDNA translocated and unwound by an individual RecBCD enzyme molecule. The reported variation is the standard deviation of the processivity for all enzyme molecules at a particular ATP concentration.
‡The number in parentheses indicates the number of DNA molecules used to determine the unwinding rates and the processivities at each ATP concentration; eight molecules were examined in the absence of ATP.

We fitted the processivity data from the same 40 molecules analysed in Fig. 3a to a hyperbolic function to determine a maximum processivity at 23 °C of 29,670 ± 4,256 bp per binding event, with an apparent $K_m^{ATP}$ for processive unwinding ($K_N^{ATP}$) of 158 ± 78 μM (Fig. 3b; and ref. 1). These results are similar to those reported previously for RecBCD enzyme using both gel and fluorescence measurements (32,000 ± 1,800 bp per end, and $K_N^{ATP}$ = 41 ± 9 μM; ref. 1). The processivity is even higher at elevated temperature, increasing to an average of 38,000 ± 5,700 bp per dsDNA end-binding event (Table 1); in fact one RecBCD enzyme molecule could unwind as much as 42,300 bp of dsDNA. As the translocation step size is 23 bp (ref. 17), a single RecBCD enzyme has the capacity to take as many as 1,840 steps (translocating a total distance of 13 μm) before dissociating when the ATP concentration is not limiting.

We have observed both the rate and processivity of dsDNA unwinding for individual RecBCD enzyme molecules using a single-molecule helicase assay. To our knowledge, this is the first time that the action of individual DNA helicase molecules on dsDNA substrates has been observed in real time. The results obtained are consistent with and in precise agreement with previously published reports[1,11,7,12]. This assay has further potential and can be used to study a variety of individual nucleic acid enzymes: both those that simply bind to nucleic acids to effect a conformational change (for example, the DNA strand-exchange protein, RecA protein, that displaces fluorescent dye molecules upon binding to dsDNA[18]), and those that process DNA in a manner similar to that observed here. □

## Methods

### Optical trapping and fluorescence microscopy

DNA helicase reactions were performed in a two-channel, Y-shaped, micro-machined glass flow cell[6] (Fig. 1) with the inlet ports connected to 1-ml syringes controlled by a syringe pump (Model KDS 200; KD Scientific, Boston, MA). The flow cell was held in place on a motorized stage controlled by an MSI-2000 computerized stage controller (0.1-μm resolution; Applied Scientific Instruments). The stage was positioned in a Nikon ES400 microscope, which was equipped for epifluorescence and modified to incorporate an optical trap. The optical trap used an Nd:YLF infrared laser (wavelength 1,047 nm, 500 mW; Spectra Physics) focused through an oil-immersion objective lens (Plan Fluor 100×, 1.3 N.A.; Nikon) and Immersol (518F, low fluorescence; a gift from Zeiss), to a position 10–15 μm below the upper surface of the flow cell. The flow cell is ~4,000 μm wide, and trapping is initially done 100–200 μm from the boundary between solutions on the sample side of the flow cell, to ensure that a trapped complex that may have a RecBCD enzyme molecule attached, has not been exposed to ATP. The trapped complex is moved

~400 μm into the reaction side to ensure that the reaction occurs in a homogenous concentration of ATP.

Fluorescent DNA–bead complexes were excited with the microscope's high-pressure mercury lamp using the appropriate filter set (blue filter set #11001; Chroma Technology, Brattleboro, VT). Fluorescence images were captured by a charge-coupled device camera (CCD-300T-IGF; Dage-MTI, Michigan City, IN) coupled to an image intensifier (VS4-1845; Video-Scope International, Sterling, VA), and were recorded on VHS videotape. To increase temperature to 37 °C, the microscope stage was enclosed in a Plexiglas housing and warm air was introduced.

### DNA–bead preparation

The protocol used was modified from ref. 6. Bacteriophage λ DNA (0.096 pmoles; New England Biolabs) was biotinylated at one end by annealing and ligating a 3′-biotinylated, 12-mer oligonucleotide (50 pmoles; Operon Technologies) complementary to one of the cohesive ends. The biotinylated λ DNA ($3.6–7.2 \times 10^8$ molecules total) was reacted with 1 μm, streptavidin-coated, polystyrene beads ($1.92 \times 10^8$ beads total; Bangs Laboratories) in 82 mM $NaHCO_3$ (pH 8.0) at 37 °C for 60 min. DNA–bead complexes were immediately transferred to a degassed solution containing 57 mM $NaHCO_3$ (pH 8.0), 30 mM dithiothreitol (DTT), 20% sucrose and 0.2 μM YOYO-1 (Molecular Probes). Dye binding was performed for a minimum of 60 min at 24 °C in the dark.

### Single-molecule DNA helicase reactions

Before use, the flow cell was coated with either casein or BSA (100 μg $ml^{-1}$). The excess, unbound protein was washed out using 100 mM $NaHCO_3$ (pH 8.0). For each assay the sample syringe contained 41 mM $NaHCO_3$ buffer (pH 8.0), 35 mM DTT, 13% sucrose, 0.133 μM YOYO-1, 2 mM magnesium acetate, $1.92 \times 10^8$ DNA–bead complexes, and 4.6 nM RecBCD enzyme. The reaction syringe contained 41 mM $NaHCO_3$ buffer (pH 8.0), 35 mM DTT, 13% sucrose, 0.02 μM YOYO-1, 2 mM magnesium acetate, and ATP at the correct concentration. The *Escherichia coli* single-stranded DNA (ssDNA)-binding protein was not needed in these reactions because endonucleolytic cleavage of unwound ssDNA by the associated nuclease activity of RecBCD enzyme, releases the ssDNA as fragments that are immediately washed away in the buffer flow and, thus, do not accumulate to either inhibit the enzyme[19] or affect the observed fluorescence signal[7].

The RecBCD enzyme preparation used in all experiments was 100% active (data not shown) as determined using a spectrofluorometric helicase assay[11]. Standard visualization reactions were done at room temperature (~23 °C) using degassed buffers. Flow was initially at 0.8 ml $h^{-1}$ for 10 min and was gradually decreased in increments of 50% to a final flow rate 10–20 μl $h^{-1}$ (linear flow rates of ~80–150 μm $s^{-1}$), over a period of ~20 min.

### Data analysis

Images were captured on a Power PC Macintosh computer interfaced with the VCR through an LG-3 frame-grabber card, operating at 1 frame per 33 ms, and controlled by Scion NIH Image v1.62c (Scion Corporation). Captured videos were converted into individual, time-stamped, sequential frames (Fig. 2) to make measurements. Individual DNA molecules were measured using the linear measurement tool of Scion NIH Image; calibration of the microscope optics was achieved using an Objective Micrometer (Fisher Scientific) that was marked in units of 10 μm.

The rate of DNA unwinding was calculated by measuring the observed length of DNA in each frame of a time course and fitting the resultant data to a linear function by least squares analysis. The resulting slope in each ATP-dependent reaction was corrected using the slope determined in the absence of ATP; this corrected slope was multiplied by the number of bp of λ DNA per μm to calculate the corrected rate in units of bp $s^{-1}$. Under the assay conditions used, the average length of individual, stretched, fluorescent λ DNA molecules was 14.9 μm ($n$ = 43), which is shorter than previously published lengths[5,6]. Those reports used a higher concentration of sucrose and were done in the absence of magnesium ions. In our experiments, the length of a single, stretched λ DNA molecule was affected by flow rate and by the concentrations of sucrose, magnesium ions, and YOYO-1, varying from nore than 18 μm in 20% sucrose in the absence of magnesium acetate, to 14.9 μm in 13% sucrose and 2 mM magnesium acetate (data not shown). Thus, for all calculations, as λ DNA is 48,502 bp in length, and the observed average length of a λ DNA molecule is 14.9 μm, the average number of bp per μm is 48,502/14.9 = 3,255.

Received 23 May; accepted 23 October 2000.


1. Roman, L. J., Eggleston, A. K. & Kowalczykowski, S. C. Processivity of the DNA helicase activity of *Escherichia coli* recBCD enzyme. *J. Biol. Chem.* **267,** 4207–4214 (1992).
2. Arnold, D. A. & Kowalczykowski, S. C. in *Encyclopedia of Life Sciences* [online] (Nature Publishing Group, London, 1999) ⟨http:///www.els.net⟩.
3. Kowalczykowski, S. C., Dixon, D. A., Eggleston, A. K., Lauder, S. D. & Rehrauer, W. M. Biochemistry of homologous recombination in *Escherichia coli*. *Microbiol. Rev.* **58,** 401–465 (1994).
4. Kuzminov, A. Recombinational repair of DNA damage in *Escherichia coli* and bacteriophage lambda. *Microbiol. Mol. Biol. Rev.* **63,** 751–813 (1999).
5. Perkins, T. T., Smith, D. E. & Chu, S. Direct observation of tube-like motion of a single polymer chain. *Science* **264,** 819–822 (1994).
6. Brewer, L. R., Corzett, M. & Balhorn, R. Protamine-induced condensation and decondensation of the same DNA molecule. *Science* **286,** 120–123 (1999).
7. Eggleston, A. K., Rahim, N. A. & Kowalczykowski, S. C. A helicase assay based on the displacement of fluorescent, nucleic acid-binding ligands. *Nucleic Acids Res.* **24,** 1179–1186 (1996).
8. Ganesan, S. & Smith, G. R. Strand-specific binding to duplex DNA ends by the subunits of *Escherichia coli* recBCD enzyme. *J. Mol. Biol.* **229,** 67–78 (1993).
9. Bennink, M. L. *et al.* Single-molecule manipulation of double-stranded DNA using optical tweezers: interaction studies of DNA with RecA and YOYO-1. *Cytometry* **36,** 200–208 (1999).
10. Taylor, A. F. & Smith, G. R. Substrate specificity of the DNA unwinding activity of the RecBC enzyme of *Escherichia coli*. *J. Mol. Biol.* **185,** 431–443 (1985).
11. Roman, L. J. & Kowalczykowski, S. C. Characterization of the helicase activity of the *Escherichia coli* RecBCD enzyme using a novel helicase assay. *Biochemistry* **28,** 2863–2873 (1989).
12. Eggleston, A. K. & Kowalczykowski, S. C. The mutant recBCD enzyme, $recB^{2109}$CD enzyme, has helicase activity but does not promote efficient joint molecule formation *in vitro*. *J. Mol. Biol.* **231,** 621–633 (1993).
13. Taylor, A. & Smith, G. R. Unwinding and rewinding of DNA by the recBC enzyme. *Cell* **22,** 447–457 (1980).
14. Xue, Q. F. & Yeung, E. S. Differences in the chemical reactivity of individual molecules of an enzyme. *Nature* **373,** 681–683 (1995).
15. Wuite, G. J. L., Smith, S. B., Young, M., Keller, D. & Bustamante, C. Single-molecule studies of the effect of template tension on T7 DNA polymerase activity. *Nature* **404,** 103–106 (2000).
16. Roman, L. J. & Kowalczykowski, S. C. Characterization of the adenosinetriphosphatase activity of the *Escherichia coli* RecBCD enzyme: Relationship of ATP hydrolysis to the unwinding of duplex DNA. *Biochemistry* **28,** 2873–2881 (1989).
17. Bianco, P. R. & Kowalczykowski, S. C. Step size measurements on the translocation mechanism of the RecBC DNA helicase. *Nature* **405,** 368–372 (2000).
18. Zaitsev, E. N. & Kowalczykowski, S. C. Binding of double-stranded DNA by *Escherichia coli* RecA protein monitored by a fluorescent dye displacement assay. *Nucleic Acids Res.* **26,** 650–654 (1998).
19. Anderson, D. G. & Kowalczykowski, S. C. SSB protein controls RecBCD enzyme nuclease activity during unwinding: a new role for looped intermediates. *J. Mol. Biol.* **282,** 275–285 (1998).


**Supplementary information** is available on *Nature*'s World-Wide Web site (http://www.nature.com) or as paper copy from the London editorial office of *Nature*.


### Acknowledgements

We would like to thank S. Chan and J. Lengyel for assistance with measurements, and the following people for their comments on the manuscript: N. Handa, J. Kleiman, A. Mazin, J. New, E. Seitz, M. Spies, T. Sugiyama and Y. Wu. This work was supported by an NIH Grant to S.C.K. and a DOE Center of Excellence for Laser Applications in Medicine Grant to Y.Y. and R.J.B.


Correspondence and requests for materials should be addressed to S.C.K. (e-mail: sckowalczykowski@ucdavis.edu).

# Crystal structure of the transcription activator BmrR bound to DNA and a drug

**Ekaterina E. Zheleznova Heldwein & Richard G. Brennan**

*Department of Biochemistry and Molecular Biology, Oregon Health Sciences University, Portland, Oregon 97201-3098, USA*

**The efflux of chemically diverse drugs by multidrug transporters that span the membrane[1] is one mechanism of multidrug resistance in bacteria. The concentrations of many of these transporters are controlled by transcription regulators, such as BmrR in *Bacillus subtilis*[2], EmrR in *Escherichia coli*[3] and QacR in *Staphylococcus aureus*[4]. These proteins promote transporter gene expression when they bind toxic compounds. BmrR activates transcription of the multidrug transporter gene, *bmr*, in response to cellular invasion by certain lipophilic cationic compounds (drugs)[2,5,6]. BmrR belongs to the MerR family, which regulates response to stress such as exposure to toxic compounds or oxygen radicals in bacteria[7–12]. MerR proteins have homologous amino-terminal DNA-binding domains but different carboxy-terminal domains, which enable them to bind specific 'coactivator' molecules. When bound to coactivator, MerR proteins upregulate transcription by reconfiguring the 19-base-pair spacer found between the −35 and −10 promoter elements to allow productive interaction with RNA polymerase[7,9–12]. Here we report the 3.0 Å resolution structure of BmrR in complex with the drug tetraphenylphosphonium (TPP) and a 22-base-pair oligodeoxynucleotide encompassing the *bmr* promoter. The structure reveals an unexpected mechanism for transcription activation that involves localized base-pair breaking, and base sliding and realignment of the −35 and −10 operator elements.**